Nuclear Instruments and Methods in Physics Research A 444 (2000) 449–452

NUCLEAR INSTRUMENTS & METHODS IN PHYSICS RESEARCH Section A

www.elsevier.nl/locate/nima

Optical/UV single-photon imaging spectrometers using superconducting tunnel junctions

C.M. Wilson[a,*], K. Segall[a], L. Frunzio[a], L. Li[a], D.E. Prober[a], D. Schiminovich[b], B. Mazin[b], C. Martin[b], R. Vasquez[c]

[a] *Yale University, New Haven, CT 06520, USA*
[b] *California Institute of Technology, Pasadena, CA, USA*
[c] *NASA Jet Propulsion Laboratory, Pasadena, CA, USA*

Abstract

We present preliminary test results of optical/UV single-photon imaging spectrometers using superconducting tunnel junctions. Our devices utilize a lateral trapping geometry. Photons are absorbed in a Ta thin film, creating excess quasiparticles. Quasiparticles diffuse and are trapped by $Al/AlO_x/Al$ tunnel junctions located on the sides of the absorber. The Ta/Al interface does not overlap the junction area. Imaging devices have tunnel junctions on two opposite sides of the absorber. Position information is obtained from the fraction of the total charge collected by each junction. We have fabricated high-quality junctions with a ratio of subgap resistance to normal state resistance greater than 100 000 at 0.22 K. We have measured the single-photon response of our devices. For photon energies between 2 and 5 eV, we measure an energy resolution between 1 and 1.6 eV. We can estimate the number of pixels the device can resolve from the energy resolution. We find that these early devices have as many as 4 pixels per strip.

PACS: 07.60.Rd; 42.79.Pw; 85.25 − j; 85.60.Gz

Keywords: Superconductivity; Spectrometer; Junction; Imaging; Detector

1. Introduction

There has been great interest in the concept of single-photon spectroscopy in recent years. Two competing technologies are superconducting tunnel junctions (STJ) and transition edge sensors (TES) [1,2]. These detectors can operate at energies ranging from the optical to the X-ray. In the optical/UV region, much attention has been focused on imaging spectrometers. The general approach pursued to date is large format arrays of single pixel detectors [3].

We propose to develop STJ detectors with intrinsic imaging, meaning that the detectors have many more pixels than read out channels. We do this using STJ detectors with lateral trapping. This work is an extension of successful X-ray work, where we have made detectors with a resolution of 26 eV referred to a 6 keV X-ray [4,5].

* Corresponding author.

PII: S0168-9002(99)01421-7

2. Operating principle

Fig. 1 shows a schematic drawing of an imaging STJ detector. Many physical processes are involved in the operation of these detectors. First, an incident photon is absorbed in the central Ta film breaking Cooper pairs and creating quasiparticles. The quasiparticles diffuse until they reach the Al. In the Al, they can scatter inelastically, losing energy until they reach the Al gap. Once the quasiparticles scatter below the gap of Ta, they are "trapped" in the Al electrode. The quasiparticles then tunnel and are read out as an excess subgap current. The current pulses are then integrated to obtain a charge from each junction, Q_1 and Q_2. We have the relation

$$Q_1 + Q_2 \propto \frac{E_{\text{photon}}}{\Delta_{\text{Ta}}},$$

where E_{photon} is the photon energy and Δ_{Ta} is the energy gap of Ta.

The fraction of charge collected in each junction tells us the location of the absorption event. If the photon is absorbed in the center, then the charge divides equally. If the photon is absorbed at one edge of the absorber, then most of the charge is collected by the closest junction. In the limit of no absorber loss and perfect trapping

$$\frac{L}{\Delta L} \geq \sqrt{2}\,\frac{E}{\Delta E},$$

where L is the length of the absorber, ΔL is the uncertainty in the position and ΔE is the uncertainty in energy [6]. ΔL is the effective size of a pixel.

Another important process in our detectors is backtunneling. Considering one half of Fig. 1, we have a lateral Ta/Al/AlO_x/Al/Ta tunnel junction. We inject excited quasiparticles into the Al from the Ta absorber. The high-Ta gap then confines excited quasiparticles near the tunnel barrier. Quasiparticles can then circulate, tunneling and backtunneling. Because both tunneling and backtunneling transfer a charge in the forward direction, we measure an integrated charge many times greater then the number of quasiparticles. This effect gives the junctions charge gain.

We have designed our devices to maximize backtunneling. We have interrupted the Al wiring with Ta plugs. The absorber and the plugs confine the quasiparticles near the junction.

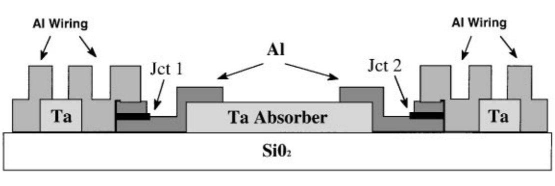

Fig. 1. Schematic of an imaging STJ detector using lateral trapping and backtunnelling. Not shown is an insulating SiO layer between the trap and wiring.

3. Experimental conditions

All devices have been fabricated at Yale in a high-vacuum deposition system with in situ ion beam cleaning. We start with an oxidized Si substrate. The Ta absorber and plugs are then sputtered at 750°C. Next, a Nb ground contact is sputtered. The Al trilayer is then evaporated in one vacuum cycle. An SiO insulating layer is evaporated and finally Al wiring is evaporated. An in situ ion beam cleaning is performed before each metal deposition to ensure good metallic contact. All layers are patterned photolithographically using either wet etching or lift-off.

Measurements are made in a two stage ^{3}He dewar. The base temperature is 220 mK.

To measure the photo-response of our junctions, we use a room temperature JFET current amplifier. We use an Amptek A250 amplifier with a 2SK146 input transistor. Extra circuitry is added that allows the A250/2SK146 to be DC coupled to the junctions [7]. The amplifier thus provides an active voltage bias for the junction.

We illuminate the detectors using a small Hg lamp calibration source. A band-pass filter is used to select one photon energy at a time. We bring light into the dewar using an optical fiber. The fiber is UV grade fused silica. The fiber is Al coated to enhance UV transmission up to energies of 6 eV. The filtered light passes through a fiber splitter that divides the light equally between two fibers. One of these fibers is fed into the dewar. The other fiber is fed into a photomultiplier tube which simultaneously measures the intensity.

4. Results

We have had success fabricating high-quality thin films. We have made Ta films with a residual resistance ratio of 17. We have also measured a quasiparticle loss time of 450 μs at 220 mK. This loss time can be compared to a time of ∼10 μs needed for a quasiparticle to diffuse across the absorber and be trapped in the Al junctions. We have made Al films with a residual resistance ratio of 12. We have measured a quasiparticle loss time of 57 μs at 220 mK in these Al films. This loss time can be compared to the ∼1 μs tunnel time in a typical junction.

We have also made outstanding junctions. Two characteristics are important for low noise. First, junctions should have a low subgap current to minimize shot noise. They should also have a large subgap resistance to minimize the contribution of amplifier voltage noise. Fig. 2(a) shows the subgap I–V curve of a 400 μm^2 junction with a normal state resistance of $R_{NN} = 2.3\,\Omega$. At 220 mK we measure a subgap current of ∼5 nA and a subgap resistance of 880 kΩ. The subgap resistance exceeds our expectations by an order of magnitude.

Unfortunately, we have not been able to completely reproduce this quality. Fig. 2(b) shows the subgap curve of a 100 μm^2 junction from a different fabrication run. This junction has a normal state resistance of $R_{NN} = 13.8\,\Omega$. In this junction the subgap resistance is only 8 kΩ. We do not understand if this difference is a fabrication issue or if it reflects a problem with the experimental setup.

We have detected optical and ultraviolet photons using a detector with junctions as in Fig. 2(b). This device has a Ta absorber 10 μm wide by 100 μm long by 0.6 μm thick. Each Al trap overlaps the absorber by 5 μm. In Fig. 3, we show two histograms of events recorded with this detector. Figs. 3(a) and (b) are the response to illumination with 4.89 eV UV photons and 2.27 eV green photons, respectively. We have plotted the number of events versus the inferred photon energy. The photon energies are inferred from the collected charge assuming the response is linear. The raw current pulses have been digitally filtered before being integrated to obtain the charge measurements.

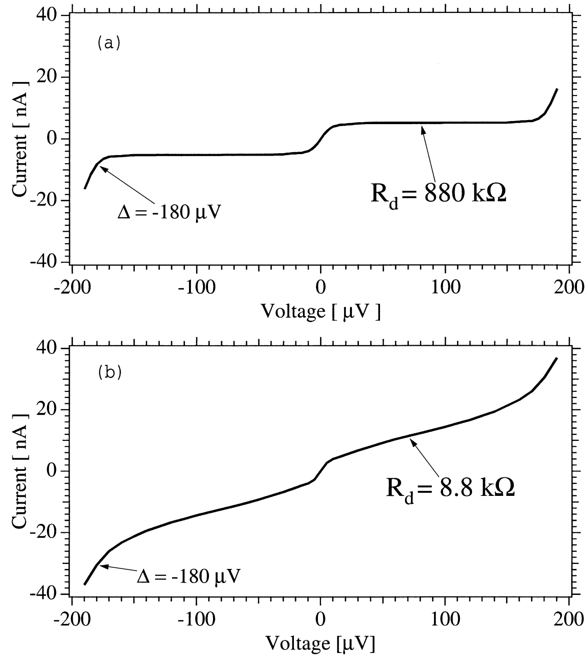

Fig. 2. Subgap I–V curves of two junctions. Both measurements are made at $T = 220$ mK. The junction parameters are: (a) area = 400 μm^2, $R_{NN} = 2.3\,\Omega$; (b) area = 100 μm^2, $R_{NN} = 13.8\,\Omega$.

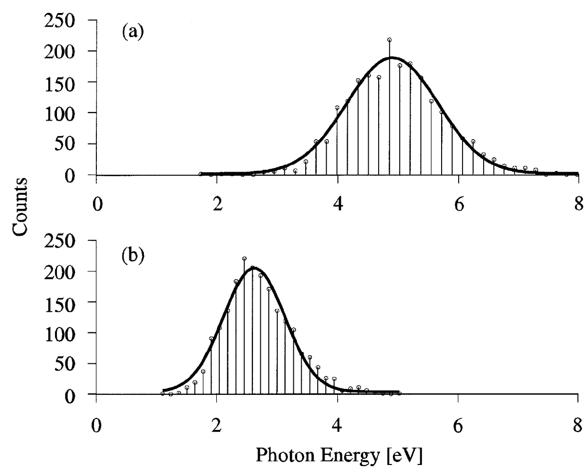

Fig. 3. Histograms of single photon events. Incident photon energies of plot (a) and (b) are 4.89 eV and 2.27 eV, respectively.

The full-width at half-maximum (FWHM) of the green histogram, measured over the full absorber, is 1.0 eV. The FWHM of the UV histogram is 1.6 eV measured over the full absorber. If only a selected range of the absorber is chosen, we obtain a FWHM of 1.1 eV for the UV histogram. We have measured the noise spectra of both junctions with no illumination and they are consistent with the measured resolution. However, the noise spectra contain excess noise that we cannot explain.

An energy resolving power of $R = 3$ in the UV implies that the detector can resolve 4 spatial pixels. This particular detector has an active absorber area 90 μm long by 10 μm wide. So, the detector has 4 pixels with dimensions 22 μm by 10 μm. This is achieved with only two readout channels.

The fall time of the photon pulses contains important physical information. We have measured the fall time by averaging 2000 single UV photon pulses and fitting an exponential to the waveform. A simple physical model tells us that the fall time of the pulse should be the quasiparticle loss time in the Al junctions. Basically, since the quasiparticles are confined near the junctions by the Ta plugs, they continue to tunnel and backtunnel until they are lost. We measure a quasiparticle loss time of $\tau_{\mathrm{loss}} = 57$ μs.

The average number of times that a quasiparticle tunnels is

$$n = \frac{\tau_{\mathrm{loss}}}{\tau_{\mathrm{tun}}},$$

where τ_{tun} is the tunnel time. We can extract the tunnel time from measurements of R_{NN}. We measure $\tau_{\mathrm{tun}} = 2.46$ μs. With this we find that $n = 23$. We also have the relation

$$Q_{\mathrm{coll}} = nQ_0,$$

where Q_{coll} is the collected charge and Q_0 is the initial charge in the junction. Combining the measured values of n and Q_{coll}, we can arrive at the initial charge from a 4.89 eV photon. We find

$$Q_0 = 7000 \pm 1100.$$

We can compare this to the theoretical value

$$Q_0 = n_{\mathrm{trap}} \frac{E_{\mathrm{photon}}}{1.7\Delta_{\mathrm{Ta}}} = 7200,$$

where the factor of 1.7 is the result of Monte Carlo calculations [8]. The number $n_{\mathrm{trap}} = 1.8$ accounts for charge multiplication upon trapping and has been measured in our X-ray detectors [9]. The two values agree within error.

5. Conlusions

We have begun the development and testing of imaging, single-photon spectrometers. Our devices use superconducting tunnel junctions with lateral trapping. Our preliminary fabrication results are very promising. We have detected single optical and UV photons with these first detectors.

References

[1] N.E. Booth, D.J. Goldie, Supercond. Sci. Technol. 9 (1996) 493.
[2] B. Cabrera et al., Appl. Phys. Lett. 73 (1998) 735.
[3] N. Rando et al., Proc. SPIE 3435 (1998).
[4] K. Segall et al., IEEE Trans. On Appl. Supercond., to appear.
[5] S. Friedrich et al., Appl. Phys. Lett. 71 (1997) 3901.
[6] H. Kraus et al., Phys. Lett. B 231 (1989) 195.
[7] S. Friedrich et al., IEEE Trans. Appl. Supercond. 7 (1997) 3383.
[8] N. Rando et al., Nucl. Instr. and Meth. 313 (1992) 173.
[9] S. Friedrich, Ph.D. Thesis, Yale University, 1997.